Journal of Optoelectronics and Advanced Materials Vol. 3, No. 2, June 2001, p. 425 - 432

STRUCTURE AND PROPERTIES OF CHALCOGENIDE GLASSES IN THE SYSTEM $(As_2S_3)_{1-x}(Sb_2S_3)_x$

F. Sava

National Institute of Materials Physics
Bucharest-Magurele, P.O. Box MG. 7, Romania

The glass system $(As_2S_3)_{1-x}(Sb_2S_3)_x$, $0 \le x \le 0.65$, has been studied by X-ray diffraction and microhardness measurements. The long-time irradiation of the samples by ultraviolet rays has been carried out and its structural effect was investigated. The substitutional model and the microphase separation model have been discarded. A new intermediate model, whose main feature is the formation of mezoscopic Sb_2S_3 clusters, has been advanced.

(Received: May 20, 2001; accepted June 7, 2001)

Keywords: Chalcogenide glass, Arsenic-antimony trisulfide, X-ray diffraction, Microhardness

1. Introduction

The chalcogenides glasses are important due to their remarkable properties, which make them useful in optoelectronics for infrared elements and devices for acusto-optic devices, for electrical switches, holography and information storage media [1,2]. Arsenic trisulfide (As_2S_3) is the most studied chalcogenide glass and deserves applications in infrared optics and optical coatings because of its excellent IR transmission, large glass-forming tendency, and resistance to moisture and chemicals [3]. Antimony trisulfide (Sb_2S_3) and the non-stoichiometric compositions (as e.g. SbS_4) prepared as thin amorphous films have found applications for information storage media [4]. A graded refractive index, which is required in some applications, may be produced in the non-crystalline As_2S_3 of both bulk and thin film forms by gradually replacing the arsenic component with chemically similar antimony atoms [5]. This approach will fail if the resultant glass crystallizes or undergoes a gross phase separation, because these phenomena cause light scattering. The glass-forming tendency is very different in As_2S_3 and Sb_2S_3. While for As_2S_3, even melt cooling by simply removing the sample from the furnace at room temperature, the glassy Sb_2S_3 can be obtained only for high cooling rates by using the so-called splat-cooling techniques [6]. A special method for getting glassy Sb_2S_3 by a conventional melt quenching method was demonstrated by Dalba et al. [7]. If Sb_2S_3 is added to As_2S_3 then the glass-forming ability of the mixture is greatly enhanced and, thus, a broad range of glassy As_2S_3-Sb_2S_3 alloys is obtained. Although the structure of the non-crystalline state in the binary system As_2S_3 and Sb_2S_3 is satisfactorily known, the atomic configuration in the alloys As_2S_3-Sb_2S_3 is controversial. Some authors interpreted the EXAFS, XANES, IR data and the Mössbauer experimental data on the atom ^{121}Sb in the frame of a model with random substitution of the arsenic atoms by antimony atoms with the formation of As-S-Sb bridges [8-11]. Other authors interpreted the IR, XRD, crystallization kinetics and optical gap data in the frame of a model with mixture of As_2S_3 and Sb_2S_3 microphases exhibiting weak interaction or without interaction at all [5, 12, 13]. The effect of the light of energy above the gap, in particular ultraviolet radiation in the system As_2S_3-Sb_2S_3 is poorly investigated. Hayashi et al. [14] have shown that in As_2S_3 and other chalcogenide glasses the UV irradiation produces a change in the optical absorption edge, two orders of magnitude higher than for the band-gap irradiation. While in the last case the photodarkening is caused by changes in atomic coordinations [14] and positions resulting from exciting lone pair electrons, in the case of UV irradiation an Auger process may take place, too, and, therefore, bond breaking or ionisation of atoms are more easy to occur, leading to layer change in local structure of the non-crystalline network. In this paper are reported the results obtained in the study of the glassy system $(As_2S_3)_{1-x}(Sb_2S_3)_x$ $0 \le x \le 0.65$ by X-ray diffraction and microhardness measurements. A structural model for the glassy materials was proposed.

2. Experimental

Glasses were prepared by melting stoichiometric mixtures of glassy As_2S_3 and polycrystalline Sb_2S_3 in sealed silica ampoules, previously evacuated at 10^{-5} Torr. Melting was carried out at 850 ºC for ~

8 hours in a rotating furnace in order to ensure homogeneity. Glasses were then obtained by water-quenching the silica ampoules. The following glassy ingots were obtained: $(As_2S_3)_{1-x}(Sb_2S_3)_x$ x = 0; 0.05; 0.25; 0.45 and 0.65.

The densities of the ingots were determined by the Archimede's method. The microhardness of the ingots were determined with a PMT-3 tester provided with diamond indentation prism. Indentation loads between 10 g and 50 g were used. The structure of the samples has been determined by X-ray diffraction in a TUR-M62 diffractometer equipped with a copper target tube. The samples were prepared by grinding chunks of ingots in a mortar and then pressing the powder in a special support to be mounted in the diffractometer. The X-ray diffraction patterns for every sample were recorded in the frame of a step by step method with the measuring time per angular position of 40s. The angular step was 0.05º. The parameters of the first sharp diffraction peak (FSDP) were carefully extracted by a computing procedure. The whole X-ray diffraction curves measured in the range 7.25º-74.25º (θ) were processed and the radial electron density distribution curves (REDD) were obtained with special computing programs written in FORTRAN language.

3. Results

3.1 Density

The exact values of the densities of the chalcogenide glasses are important both for the computation of the radial electronic density distribution curves and for the explanation of the photostructural effects which are in many cases accompanied by volume changes [15,16].

Moreover, in order to check various models of the atomic scale structure it is necessary to have accurate determinations of the material density.

The densities of the glassy ingots have been determined by the Archimede's method. Special attention was paid to the elimination of air bubbles during immersion in water. The accuracy of the mass determination was ±0.0001g, and the accuracy of the densities was ±0.01g/cm^3. The results are shown in Fig. 1.

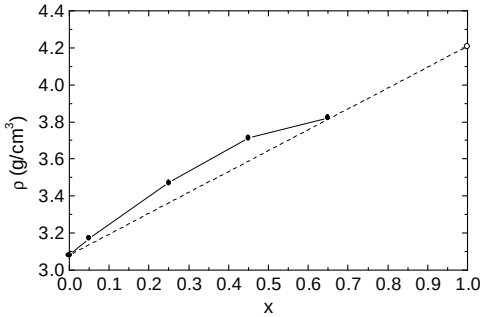

Fig. 1. -●- The density of the glassy samples in the system $(As_2S_3)_{1-x}(Sb_2S_3)_x$;
--- Theoretical densities in the case of phase mixture (As_2S_3 and Sb_2S_3).

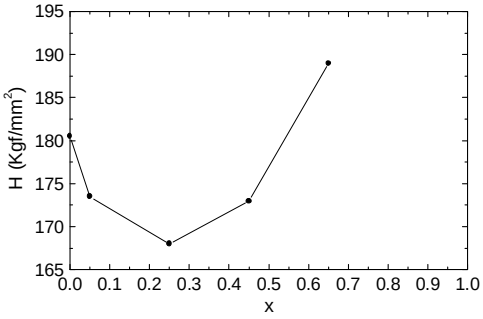

Fig. 2. The microhardness in the glassy system $(As_2S_3)_{1-x}(Sb_2S_3)_x$;

While the theoretical curve for the case of the mechanical mixture of two phases (As_2S_3 and Sb_2S_3) corresponds to the linear variation with x of the densities, the experimental values show a significant deviation from the linearity in the glass-forming region. This effect speaks in favour of the preserving of the basical structural arrangement of As_2S_3 during alloying with Sb_2S_3 for the range of the possible glassy state in the system As_2S_3-Sb_2S_3 for the range of glassy alloys. For x = 0.65 the density of the sample approaches that corresponding to a mixture of arsenic and antimony based sulfides. The Sb_2S_3 density was that reported in [6].

3.2. Microhardness

One of the parameters, which offer informations on the strength of the interatomic bonds, is the microhardness. The microhardness of the glassy ingots was determined with the help of a PMT-3 microhardness tester provided with diamond indentation prism. The tester gives the hardness in Vickers (Kgf/mm^2) or in gigapascals (GPa). The hardness values of the glassy samples in the system As_2S_3-Sb_2S_3 are situated in the range 120-190 kgf/mm^2). Large number of indentations (20-30) has

been performed for 50 g load. The mean value of the hardness was taken as the experimental value. An accuracy of ± 5 Kgf/mm^2 was estimated from the distribution of the measured hardness values. Fig. 2 shows the glass microhardness in the system As_2S_3-Sb_2S_3 as a function of Sb_2S_3 concentration.

Hardness measurements involve complex flow mechanisms; the observed increase of hardness with x indicates structural changes leading to smaller molecular or configurational mobility.

3.3 X-ray diffraction

3.3.1 First sharp diffraction peak

The X-ray diffraction patterns of the chalcogenide compounds and alloys exhibit as a fundamental feature a narrow diffraction peak situated at low diffraction angles. Figure 3 shows the experimental X-ray diffraction curves, smoothed and aligned in order to evidence the changes produced when antimony substitutes arsenic in glassy alloys. A strong decrease of the first peak with the composition x is observed.

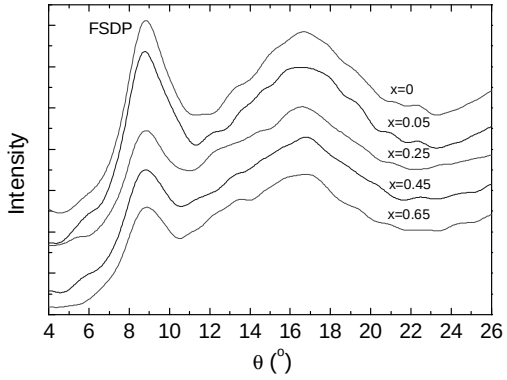

Fig. 3. X-ray diffraction patterns for glassy samples in the system $(As_2S_3)_{1-x}(Sb_2S_3)_x$.

This first sharp diffraction peak (FSDP) was explained as a "signature" of the medium range or intermediate-range order in the non-crystalline matrix. In the investigated compositions FSDP exhibits significant modifications a function of antimony content. Three parameters have been carefully measured: the peak area, peaks position on the angular scale and peak width. The last two parameters allow for calculation of the quasi-periodicity, d, and the correlation size, D, in the material, respectively. Fig. 4 shows the results.

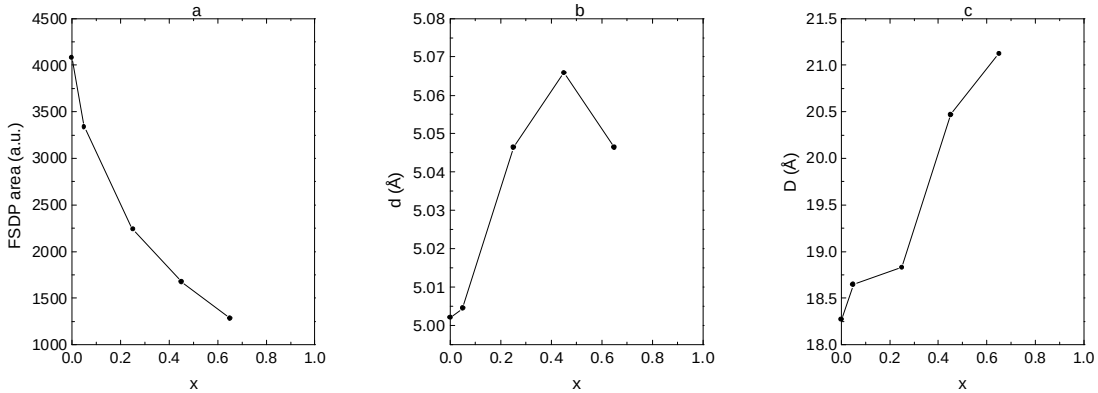

Fig. 4. The evolution of FSDP characteristics when As atoms are substituted by Sb in the glass-forming domain of the pseudo-binary system $(As_2S_3)_{1-x}(Sb_2S_3)_x$.
a- FSDP integral intensity (area); b- Quasi-periodicity, d; c- Correlation length, D.

The area of the FSDP strongly decreases with x. The quasi-periodicity in the glass raises up to x = 0.45, then decreases. The correlation length, that is related to the range of ordering of large configurational entities increases with x.

3.3.2 Radial electron density distribution (REDD)

The method based on the calculation of the so-called radial distribution function is the most powerful technique used to determine the local structure of non-crystalline materials.

The measured X-ray diffraction intensities for the largest possible angular theta range (7.25-74.25)° were corrected for polarization and then converted into electron units. The reduced interference function i(Q) where $Q = (4\pi\sin\theta)/\lambda$ was calculated from the corrected and converted I, as follows:

$$i(Q) = \frac{I - \langle f^2 \rangle}{\langle f \rangle^2} \quad (1)$$

where <f> stands for the mean atomic scattering factor averaged over the atomic concentrations.

By a Fourier transformation of Qi(Q) the correlation function G(r) is obtained:

$$G(r) = \frac{2}{\pi} \int_0^{\infty} Qi(Q) \sin(Qr) dQ \quad (2)$$

Both the REDD(r) and the pair distribution function, g(r), can be calculated;

$$\text{REDD}(r) = 4\pi r^2 \rho_o + rG(r) = 4\pi r^2 \rho_o g(r) \quad (3)$$

where ρ_0 is the mean electronic distribution density. The Fourier transformation was carried out in the range Q = 1.03 to Q = 7.84 $Å^{-1}$.

Fig. 5 shows the REDD curves obtained for the investigated glassy composition.

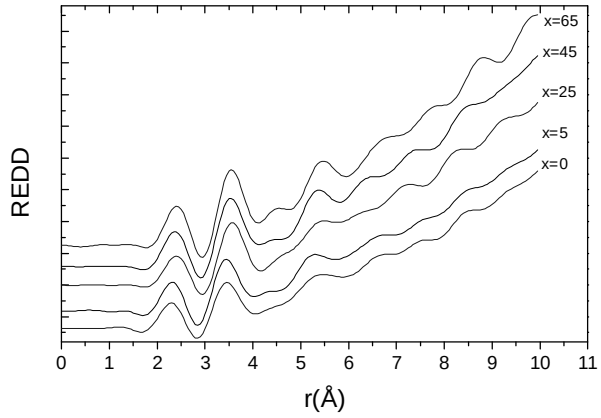

Fig. 5. The radial electron density distribution curves in the system $(As_2S_3)_{1-x}(Sb_2S_3)_x$ $\lambda_{CuK\alpha}$=1.54 Å. Integration range: 1.03 ÷ 7.84 $Å^{-1}$.

The most important characteristic of the REDD curves are related to the position, area and breadth of the first 3-4 peaks.

Careful analysis of the REDD curves allowed for getting the numerical data in Table 1.

Table 1. The most important characteristic of the REDD curves in the system $(As_2S_3)_{1-x}(Sb_2S_3)_x$.

Sb_2S_3 (x)	First coordination peak			Second coordination peak			r_2/r_1
	r_1 (Å)	Half breadth $\sigma(r_1)$	Area (u.e.)	r_2 (Å)	Half breadth $\sigma(r_2)$	Area (u.e.)	
0.00	2.250	0.588	1456	3.460	0.600	3827	1.538
0.05	2.274	0.558	1493	3.451	0.584	3984	1.518
0.25	2.349	0.606	2005	3.563	0.597	5227	1.517
0.45	2.325	0.597	2156	3.539	0.617	5628	1.522
0.65	2.361	0.587	2407	3.55	0.577	6093	1.504

4. Discussion and structural model

X-ray diffraction data have been reported for As_2S_3 glass by a number of workers [17, 18].

There is general agreement that the As-S bond length is similar to that in the crystal and that the radial distribution functions are consistent with three fold coordination of sulfur atoms about arsenic atoms. Yhe existence of a sheet-like structure in the glass has been suggested on the basis of the correspondencin position of the FSDP and the (020) reflection of orpiment (c- As_2S_3), but there is no feature in the RDF for the glass corresponding to the cross ring c_0 distance in the crystal, showing that the sheets are more or less disordered in the glass. Chemical and difraction studies on a variety of glass compositions in the arsenic-sulfur system [18] have shown that the presence of arsenic in excess of the As_2S_3 composition increases the layer separation in glass, while sulphur in excess gives rise to discrete S_8 rings.

The crystalline structure of Sb_2S_3 is a complex one. Atoms forms thread-like molecules, neighbouring molecules are coupled to form a ribbon along the b axis. The band themselves are combined into layers (double ribbons) which are parallel to the b-axis. The double ribbons have the composition $(Sb_4S_6)_n$. The ribbons represent deformed positions of a rock salt structure, somewhat reminiscent of the SnS structure. The coordination number of the Sb atoms is hard to define, it is at least three [19].

For the Sb_2S_3 glass, Zacharov and Gerasimenko [20] reported the number of S(Sb) atoms surrounding a Sb(S) atom as 4(2.7). The higher coordination numbers that in the corresponding crystalline phase were explained as a result of the absent atoms at the distances 3.15 Å and 3.20 Å which reflects the manner of joining Sb-S-Sb-S … chains into ribbons.

Tatarinova [21] has shown from electron diffraction data on thin Sb_2S_3 amorphous films that the number of S(Sb) atoms surrounding a Sb(S) atom was 6(4). A dense octahedral packing of Sb and S atoms was proposed. Resetnik [22] reported coordination numbers 5.9(3.95) for an amorphous Sb_2S_3 film.

As regarding the system As_2S_3-Sb_2S_3 Tichý et al. [23] have shown that in the first approximation it is a nearly ideal solution of the As_2S_3 and Sb_2S_3 microstructural species, while Kawamoto and Tsuchihashi [12] concluded from the results of the study of the various properties and structure of glasses that the structure is composed of As_2S_3 and Sb_2S_3 regions which are joined together by linkages like As-S-Sb. On the other hand Vinogradova [24] has shown from the diagram of state that in the system takes place eutectic interaction because the eutectics is degenerated. The system do not have solid solution region, nor ternary compounds. The liquidus curve shows the tendency to separation in the system [24].

The FSDP measures the spacing in layered molecular clusters (quasi-periodicity) or can be associated with certain forms of long-range order in the structure [25]. The ordering of the quasi-layers is measured by the correlation length, D. The increase of D with x shows an increasing ordering when Sb_2S_3 is added to As_2S_3.

The quasi-periodicity increases up to x = 0.5 (Fig. 3.b). This seems to be the limit of insertion of Sb into the As_2S_3 network (by substituting As). Then Sb dominates and so the typical Sb_2S_3 structure imposes its pattern to the amorphous alloy.

It is remarkable that the REDD curves (fig.5) show a well evidenced peak at distances as high as ~5.5 Å and this MRO feature can be related to the particular feature in the diffraction pattern at the position of FSDP.

The above described features can be related to the evolution of density with x. The deviation of ρ from the linear low corresponding to the model with phase separation can be explained by the model with substitution of As by Sb when the As-S bonding length becomes smaller as shown by Durand et al. [26] (from 2.286 Å for x = 0 to 2.283 Å for x = 0.75). So, the density becomes higher than for the case of simple substitution. For x>0.5 the density tends to the value with a mixture of glassy microphases: As_2S_3 and Sb_2S_3.

The weak diminishing of microhardness when the Sb_2S_3 is added can be interpreted as a bond weakening during As substitution by Sb. For higher content of Sb x>0.45 the prevalence of Sb_2S_3 microphase, increases the microhardness (as observed in Fig. 2). Further insight into the structure of As_2S_3-Sb_2S_3 glassy systems can be obtained from the REDD curves.

The position and the area under first peak (r_1 and A_1) gives information on the first atomic coordination sphere in the system. Fig. 6a and 6b shows the evolution of the position of the first atomic coordination in the system and of the area (in electronic units) compared to the theoretical data assuming a linear variation of these parameters with the composition (the case of a phase mixing in the system).

The electron density data for As_2S_3 and Sb_2S_3 in the first coordination sphere were calculated for the case of 3-fold and four-fold coordination of As and respectively Sb in the frame of a random covalent model, according to the formulas:

$A_3 = 2[3xZ_{As}Z_S + (1-2x)Z_S^2]$

$A_4 = 2[2x^2Z_{Sb}^2 + (1-x)^2Z_S^2 + 3x(1-x)Z_{Sb}Z_S]$

where Z_{As}, Z_{Sb}, and Z_S are the number of electrons on As, Sb and S, respectively.

From Fig. 6 we may conclude that antimony enters into the alloy with a coordination number higher than 3. The second peak in REDD curves gives the distances directly related to the bond angle on As, Sb and S atoms.

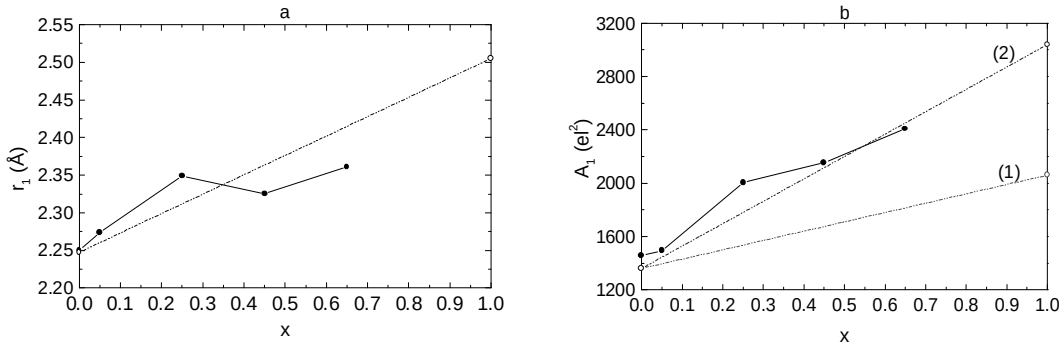

Fig. 6. First coordination (position (a) and magnitude (b)) in the system $(As_2S_3)_{1-x}(Sb_2S_3)_x$ from REDD.

-●- experimental data;

-○- (a) data from literature [6];

-○- (b) calculated values for three coordinated atoms As and Sb (case 1) and three-coordinated As and four-coordinated Sb atoms (case 2).

Fig. 7 a, b shows the experimental numerical values for the position and area of the second peak of REDD, together with the calculated data and those from literature.

The second coordination peak in the system follows the general trend of increasing with x. Nevertheless the lower values in the glass-forming region speak in favour of a more distortion of the basical pyramidal configurations As-S_3 and Sb-S_3 that lead to lower bonding angle on the atoms. This feature is correlated with the higher density of glassy alloys.

The area under the second peak (A_2) can be compared with the theoretical curves for three cases, as calculated in [6]:

case C: crystalline-like radial distribution (Sb_2S_3);

case L: layer-like radial distribution based only on interlayer distances (Sb_2S_3);

case B: band-like radial distribution based only on interband distances (Sb_2S_3).

In the case C, Sb has as second neighbours 8 Sb atoms in an anisotropic coordination; in the case L a highly anisotropic second coordination with 6 Sb do exist; in the case B a Sb atom is coordinated to 4 Sb atoms in the second coordination sphere. It is remarkable that our experimental points are situated near the layered case. It must be concluded that the real amorphous structure is consistent with a model with configurations similar to those in crystalline Sb_2S_3. In the same time glassy Sb_2S_3 can be classified as different if compared to the layered structure of As_2S_3 and more closed to the continuous random structure of the type As_2Te_3.

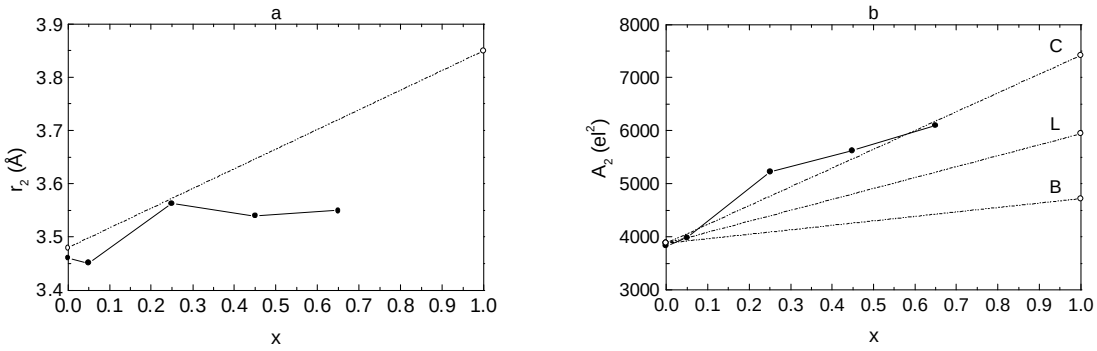

Fig. 7. The position and area of the second peak in REDD compared with the theoretical models (-o- data from literature [6]).

The amount of disorder in the system can be investigated by means of the half breadth (σ) of the distance distribution in the coordination spheres, as resulted from REED.

Fig. 8 shows the widths of the coordination spheres for the investigated samples in the system. The width of both coordination remains practically unchanged when Sb_2S_3 is added to As_2S_3.

No significant modification of MRO is produced when x increases, as proved by the decreasing tendency of σ.

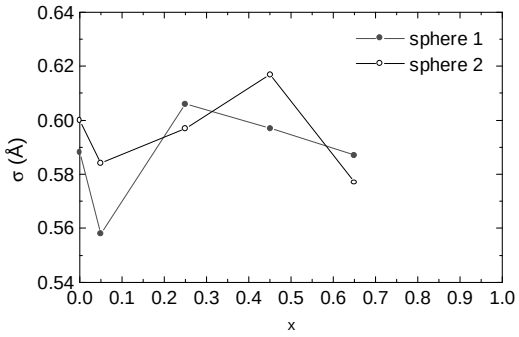

Fig. 8. The variation with x of the breadths of the first two coordination spheres in the system $(As_2S_3)_{1-x}(Sb_2S_3)_x$.

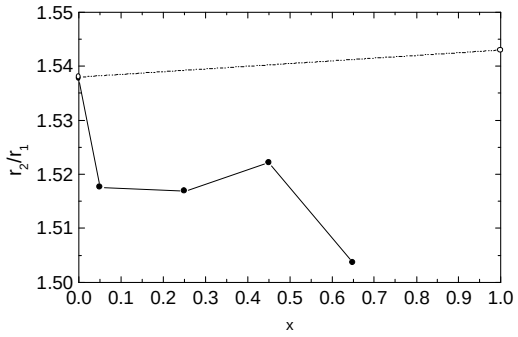

Fig. 9. The evolution of the ratio r_2/r_1 in the system $(As_2S_3)_{1-x}(Sb_2S_3)_x$ -o- data from literature.

The mechanism of transition from layered to continuous random network with x can be understood on the basis of Fig. 9. In this figure is plotted the ratio of the position of the first two coordination spheres for various x.

It is remarkable the general tendency towards lowering of the bond angles in the glassy system when Sb is added. The non-orpiment configurations develop up to x = 0.65. As-S-Sb bridges lead to chain branching and folding and to the interconnections of layer-like As_2S_3 configurations.

From infrared reflectance spectrometry Kapoutsis et al [27] have found that the destruction of As-S-As bridges with increasing Sb_2S_3 content is accompanied by the creation of mixed As-S-Sb bridges, which reach maximum abundence at x = 0.45. After x = 0.65 the Sb_2S_3 configurations dictate the structure, and the ratio r_2/r_1 increases up to Sb_2S_3 value.

5. Conclusions

The system As_2S_3-Sb_2S_3 in glassy form represents an interesting transition from the layer-like structure of As_2S_3 that incorporates step by step more Sb atoms on the As sites to continuous random structure similar to As_2Te_3 structure. The transition to three dimensional structure (at x = 0.45) is accompanied with a more and more advanced separation of Sb_2S_3 clusters. Therefore, the transition with x signifies the formation of a more homogeneous structure at the atomic scale, although clusters of Sb_2S_3 bands are practically sandwiched with As_2S_3 fragments.

The intercalation of Sb atoms into the As_2S_3 layer up to saturation is proved by the increase of the quasi-periodicity. The intercalation of Sb_2S_3 configurations is proved by the decrease of the FSDP area. A model with disordered configurations, intermediary between the Sb_2S_3-like compacted bands where some As are included, and layer-like configurations, seems to be realistic for this system.

Acknowledgements

The author are indebted to the "Horia Hulubei" foundation for financial support. He wish to thank Prof. Dr. Mihai Popescu for continuous interest and help with this paper.

References

[1] A. B. Seddon, J. Non-Cryst. Solids **184**, 44 (1985).
[2] M. Popescu, Non-Crystalline Chalcogenides, Chapter 4, Kluwer Academic Publishers, Solid State and Technology Library, Volume 8, (2000).
[3] D. R. Uhlmann, N. I. Kreidl, Glass Science and Technology, Vol.1, Glass-forming systems, Academic Press, New York (1983).
[4] A. Madan, P. Shaw, The Physics and Applications of Amorphous Semiconductors, Academic Press, New York (1988).
[5] K. White, R. L. Crane, J. A. Snide, J. Non-Cryst. Solids **103**, 210 (1988).
[6] L. Červinka, A. Hrubý, J. Non-Cryst. Solids **48**, 231 (1982).
[7] G. Dalba, P. Fornasini, G. Giunta, E. Burattini, A. Tomasi, J. Non-Cryst. Solids **97&98**, 411 (1987).
[8] M. A. El Idrissi Raghni, P. E. Lippens, J. Olivier-Fourcade, J. C. Jumas, J. Non-Cryst. Solids **192&193**, 191, 364 (1995)
[9] J. M. Durand, P. E. Lippens. J. Olivier-Fourcade, J. C. Jumas, M. Womes, J. Non-Cryst. Solids **194**, 109 (1996).
[10] E. Bychkov, G. Wortmann, J. Non-Cryst. Solids **159**, 162 (1993).
[11] M. Kato, S. Onari, T. Arai, Jap. J. Appl. Phys. **22**, 1382 (1983).
[12] Y. Kawamoto, S. Tsuchihashi, Yogyo-Kyokai-Shi **77**, 328 (1969).
[13] L.Tichy, A. Triska, M. Frumar, H. Ticha, J. Klikorta, J. Non-Cryst. Solids **50**, 311 (1982).
[14] K. Hayashi, D. Kato, K. Shimakawa, J. Non-Cryst. Solids **198-200**, 696 (1996).
[15] B. Singh, S. Rajagopalan, P. K. Bhat, D. K. Pandhya, K. L. Chopra, J. Non-Cryst. Solids, **35&36**, 1053 (1980).
[16] M. D. Mikhailov, E. A. Karpova, Z. Cimpl, F. Kosek, phys. stat. sol. (a) **117**, 467 (1990).
[17] A. A Vaipolin, E. A. Porai-Koshits, Fiz. Tv. Tela (russ.) **5**, 178 (1963).
[18] S. Tsuchihashi, Y. Kawamoto, J. Non-Cryst. Solids **5**, 286 (1971).
[19] F. Hulliger, Structural chemistry of layer-type phases, Ed. F. Lévy, D. Reidel Publ. Dordrecht-Holland/Boston-USA, 1976, p.65.
[20] V. P. Zacharov, V. S. Gerasimenko, Structure and properties of semiconductors in amorphous state (russ.), Izd. Naukova Dumka, Kiev, 1976, p.124.
[21] L. I. Tatarinova, Electronography of amorphous materials (russ.), Izd. Nauka, Moscow, 1972, p.61.
[22] A. M. Resetnik, Kristalografia (russ.) **4**, 926 (1959).
[23] L. Tichý, A. Tříska, M. Frumar, H. Tichá, J. Klikorka, J. Non-Cryst. Solids **50**, 371 (1982).
[24] G. Z. Vinogradova, Glass formation and phase equilibrium in chalcogenide systems (russ.), Ed. Nauka, Moscow, 1984.
[25] J. C. Philips, J. Non-Cryst. Solids **43**, 37 (1981).
[26] J. M. Durand, P. E. Lippens, J. Olivier-Fourcade, J. C. Jumas, J. Non-Cryst. Solids **192&193**, 364 (1995).
[27] J. A. Kapoutsis, E. I. Kamitsos, I. P. Culeac, M. S. Iovu, in Physics and Applications of Non-Cryst. Semic. in Optoelectronics, Kluwer Acad. Publ. 1997, p. 307.